

II. PHOTOSPHERIC FINE STRUCTURE

High Resolution Observations of the Photosphere

A. M. Title, R. A. Shine, T. D. Tarbell, K. P. Topka
Lockheed Palo Alto Research Laboratory
3251 Hanover Street, Palo Alto, California 94304, USA
and G. B. Scharmer
Stockholm Observatory, S-133 00 Saltsjöbaden, Sweden

ABSTRACT. High resolution observations, theoretical models, and simulations are discovering many new and exciting phenomena in the solar atmosphere. In recent years, there have been a number of very high quality observations of the solar surface and lower photosphere made on the ground at Sacramento Peak Observatory, Pic du Midi, and at the Swedish Solar Observatory, La Palma. In space the Solar Optical Universal Polarimeter (SOUP) has made diffraction limited (30 cm aperture) time sequences completely free from atmospheric disturbances. The recognition that significant progress is possible in non-linear dynamics has encouraged a number of theoretical groups to attack the problem of convection in the solar atmosphere. Two, two and a half, and three dimensional simulations yield the geometry of the flow below the surface and a prediction of the response of the atmosphere above the surface. Models of magnetic flux tubes are now very sophisticated, and modern high resolution observations should be able to test these theories. The development of the technique of Local Correlation Tracking (LCT) has allowed the direct measurement of horizontal velocities in the atmosphere near disk center. The combination of Doppler and LCT measurements allows a direct measurement of the photospheric vector flow field. Measurements from SOUP, Sacramento Peak, Pic du Midi, and La Palma have shown that mesoscale flows cover the surface and that there exist still larger scale flows associated with emerging pores and active regions. Much of the recent experimental and theoretical progress in processing and understanding high resolution data has resulted from the availability of powerful scientific workstations for user interaction, large amounts of memory for image storage, and supercomputers for the massive fluid dynamics calculations. We are now in the very early stages of learning how to use these new computer tools to identify and follow processes in the solar atmosphere.

1. Introduction

High resolution observations of the Sun are now yielding important insights into

the basic physical processes of convection, magnetic field structure, and the interactions between magnetic and velocity fields. The development and operation of new telescopes, observing techniques, camera systems, and computer systems with mass storage and interactive image displays are responsible for this progress.

The past few years has seen the completion of a number of new telescopes in the Canary Islands, Spain. Although only in their first years of operation, results of exceptional quality have already been produced. Figures 1 (a), (b), and (c) show images of quiet sun (a) and penumbra (b) taken at the Swedish Solar Observatory (SSO) and a spectrum (c) from the Vacuum Tower Telescope of the Federal Republic of Germany. Further development of these observatories and their instrumentation will occur as they come into full operation. In addition more telescopes for the Canary Islands are either under construction or in the planning stage. These include the French Themis and the Utrecht Open Tower Telescope. In the more distant future the 2.5 meter Large Earth based Solar Telescope (LEST), whose site has not as yet been selected, will greatly increase the potential for obtaining high resolution data from the ground.

On August 5 and 6, 1985 the Solar Optical Universal Polarimeter (SOUP) mounted on the European Space Agency's (ESA) Instrument Pointing System (IPS) in the United States Space Shuttle collected about 6000 diffraction limited (30 cm aperture) images of the solar surface. Because of the short orbital observing day, the time sequences are limited to 30 – 45 minutes. These sequences are pointed stably to 0.003 arc second root mean square (RMS) and are completely free from atmospheric blurring and distortion. Besides being a valuable scientific asset for studies of granulation, sunspots, and pores, they provide a baseline for evaluation of new data analysis techniques for ground based data.

Similar results can also be obtained by high altitude balloon flights. However, even at 35 to 40 km there is sufficient atmosphere to degrade images, if the telescope is not well designed thermally. SOUP will be reflown on balloons during the Max '91 period. The later half of the next decade should see the flight of the Orbiting Solar Laboratory (OSL), which includes 1 meter optical, 30 cm UV, and 30 cm XUV telescopes which feed filtergraphs, spectroheliographs, and spectrographs. OSL is a free flying polar - orbiting satellite which will have uninterrupted solar observations for approximately 240 days per year. The design life of OSL is three years and it should operate at least partially for a decade.

In the instrument area narrowband filter systems have been developed that are tunable over a broad spectral range (3500–6800 Å) and have bandpasses as narrow as 20 milliangstroms. New spectrographs with spectral resolutions of 500,000 and more are demonstrating spatial resolution of 0.3 arc seconds. Initial experiments with IR arrays show great promise for exploring the deep photosphere and the temperature minimum region and for directly measuring magnetic field strengths.

Agile mirrors (tilt correction) are in regular use in several observatories. When the seeing is good, an agile mirror can remove a sizable fraction of the wavefront error. Of course, they also remove virtually all drive errors and shake introduced

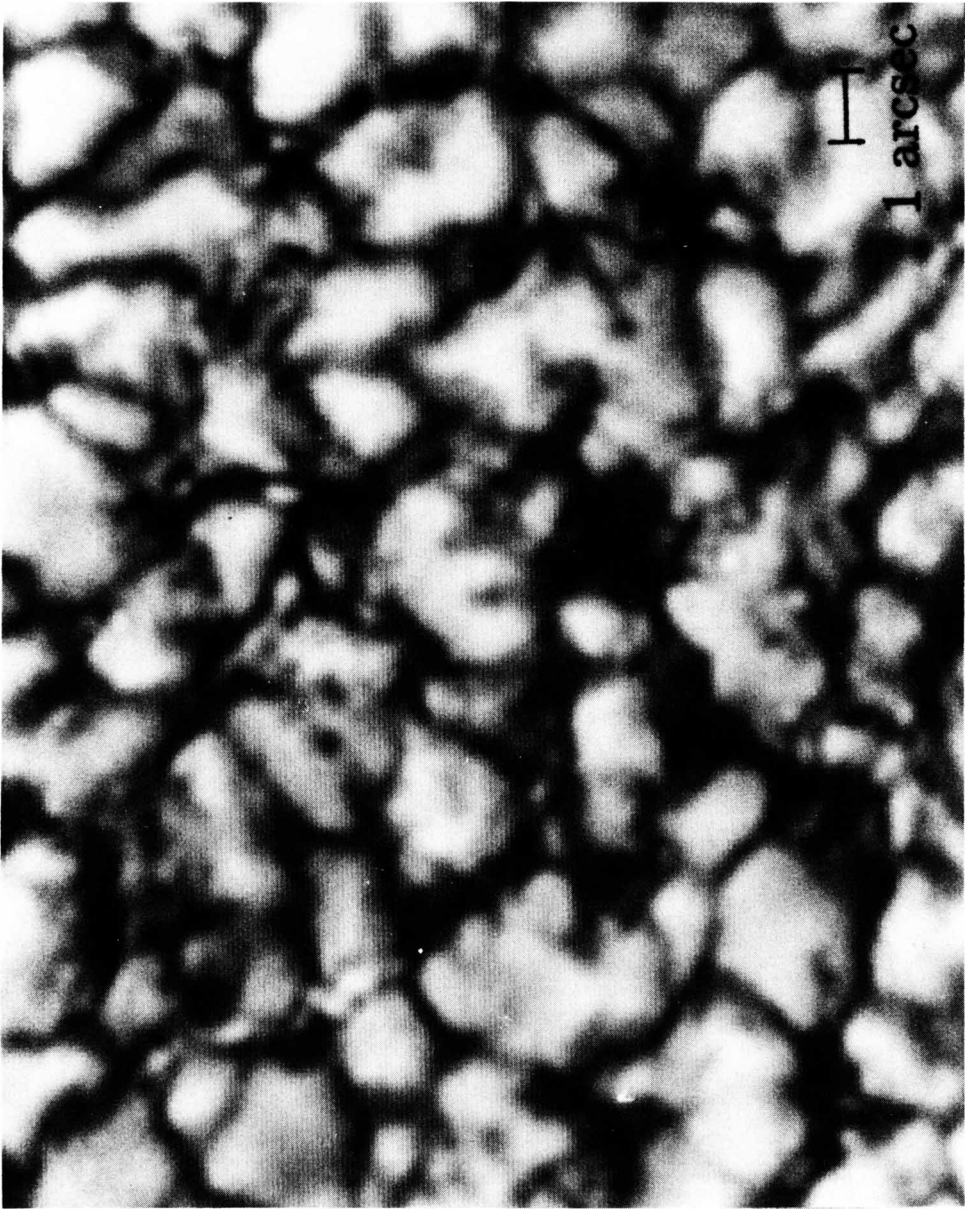


Fig. 1 (a) Image of quiet sun taken at Swedish Solar Observatory, La Palma.

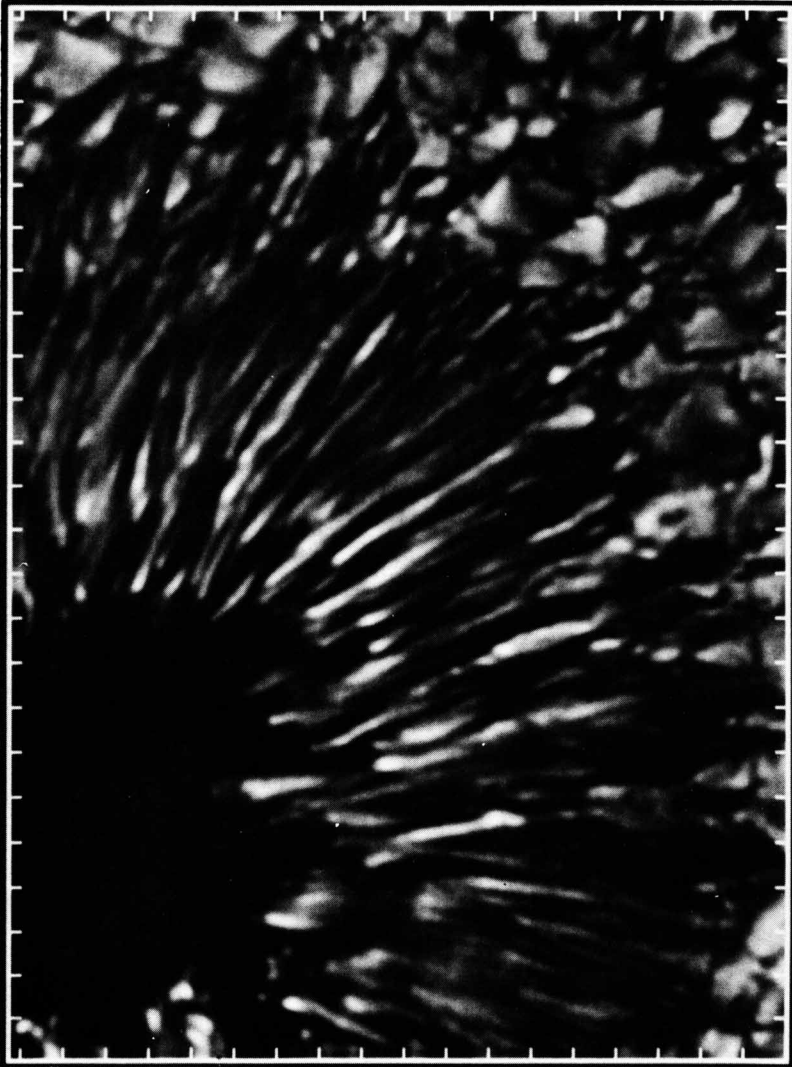


Fig. 1 (b) Image of penumbra taken at the Swedish Solar Observatory. Tick marks are at 1 arc second intervals.



Fig. 1 (c) Images of Solar Spectrum near Iron 6302 taken at the Vacuum Tower Telescope of the Federal Republic of Germany on Tenerife.

by the telescope itself. Measurements have shown that there is sufficient power in atmospheric turbulence to degrade images at frequencies as high as 100 Hz. Control signals for agile mirrors are generated by quadrant photodetectors operating on spots, pores, or the vertices in intergranular lanes. Several groups have developed correlation trackers to generate the control signal, but these are still in the test phase.

An adaptive mirror (wavefront correction) was successfully operated at the National Solar Observatory/Sacramento Peak by the Lockheed group in the summer of 1988. This technology should allow future diffraction limited observations over regions of at least a few arc seconds and significant improvement over perhaps 10 arc seconds. Figure 2 illustrates the improvement achieved by the Lockheed mirror. Measurements at Sacramento Peak and SSO indicate that, during periods of good seeing, the variations are caused by a combination of weak turbulence at high altitudes (about 10 km) and rather stronger turbulence much nearer the ground. In such situations an adaptive mirror may yield significant corrections over regions of arc minutes.

At the same time, as the capabilities for collecting high resolution data are expanding rapidly, the potential for reduction and analysis is also increasing. Solar observatories are making the transition from photographic film to solid state arrays. Detectors with 512×512 pixels are commonly available and at least one manufacturer sells detector systems with 1024×1024 pixels. It is reasonable to expect that 2048×2048 and even 4096×4096 camera systems will come in to use in the next few years.

Currently a combination of data transfer rate and storage capacity of mass memory systems limit some applications of digital camera systems. Each time a 1024×1024 camera is read with 12 bit per pixel accuracy, 12×10^6 bits must be stored. One read per second implies a system transfer rate of 1.5 megabytes per second and a storage capacity of 5.4 gigabytes per hour. This combination of high transfer rate and high capacity is currently beyond the state of the art in commercial devices which are relatively inexpensive. But it is now possible to collect 1024×1024 arrays at an average rate of one every 6 seconds and store 1500 such images or nearly 2.5 hours of observations on a single 8mm video cassette using a recorder which costs about \$5000. Laser disk video recorders allow rapid and very agile viewing of the data.

When data are taken in digital form, computers can be used to extract physical parameters directly. This is in marked contrast to the very recent past where the first step in quantitative analysis was microdensitometry of many film frames. (In fact the new CCD's can be used to reduce considerably the problem of digitizing film.) Once an image sequence is in the computer, a range of processes can be applied. These include removal of atmospheric distortions, image differencing and ratioing, local correlation tracking to measure horizontal velocities, 3D Fourier filtering to eliminate or isolate particular classes of waves, overlays of simulations or predictions on movies, and overlays of movies on movies to name but a few. These

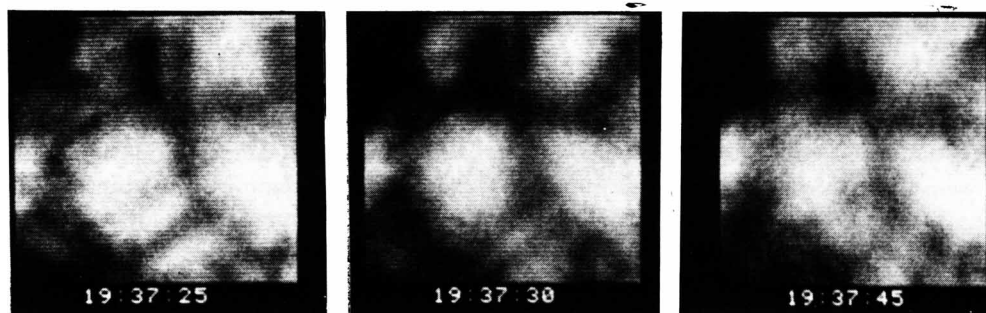
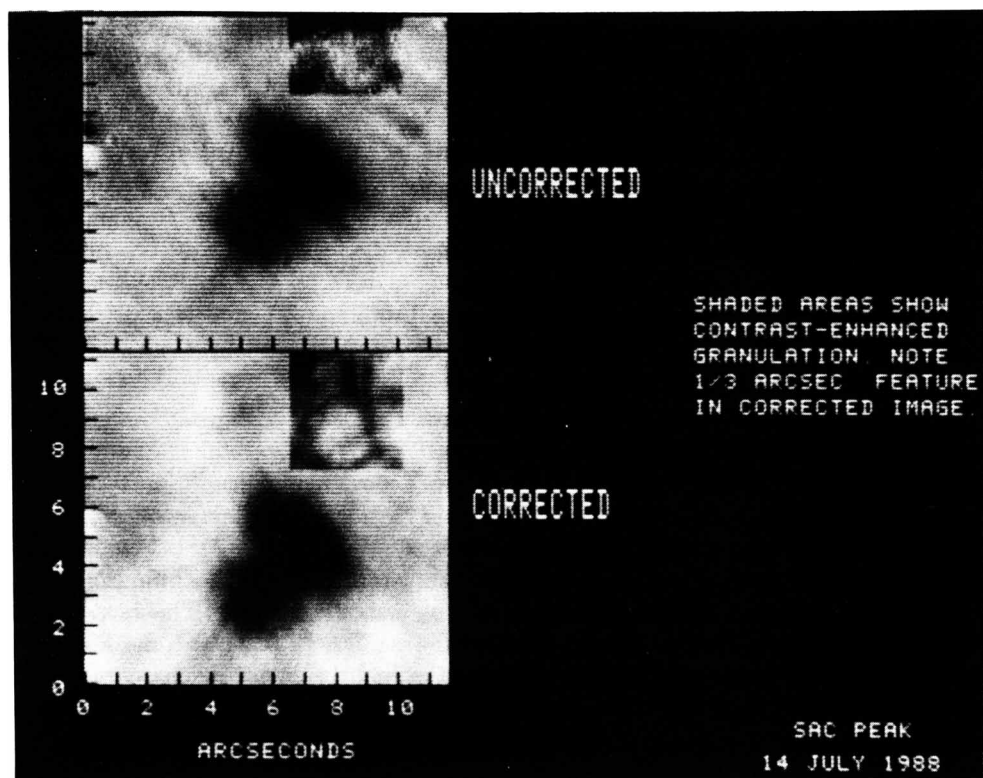


Fig. 2 Corrected and uncorrected granulation images which illustrate the improvement achieved by the Lockheed adaptive mirror at Sacramento Peak Observatory. Shown in the bottom of the figure are images from the corrected field of view. The region is 4.5 arcseconds square.

data manipulation techniques are now possible on workstation class computer systems with high resolution data displays and several gigabytes of mass storage.

In parallel with the new high resolution observations there have been significant advances in theory and simulation of solar phenomena. There are now detailed models of small flux tubes which can be tested against observations of magnetic fields, velocity fields, and line and continuum intensities. Simulations of granulation are now making predictions of phenomena in and above the surface. Predictions are also made about flow below the surface. These may be tested by using a combination of helioseismological techniques and measurements of surface flows. Progress in non-linear dynamics, Chaos theory, is yielding new insights into convection, turbulence, and dynamo generation of large and small scale magnetic fields.

In the sections below we will discuss some of the more recent and interesting discoveries using high resolution observations.

2. Continuum Observations

Over the past several decades the solar observatory on Pic du Midi has produced the very highest quality images of the solar surface. The basic technique for data collection has been to take periodic bursts of images on film. The best images in these bursts are then manually selected for study. Recently at the SSO, this process has been automated and implemented in real time. A video camera records an image every 20 milliseconds and a seeing monitor evaluates the image quality on every video field. The image and image quality value are stored in fast computer memory, so that the "best" image in a chosen time interval, typically 5–10 seconds, can be saved. This process captures the best image in sequential intervals. The only difficulty with this approach is that the time interval between images varies. But the immense advantages are that a quality movie is available in real time and all the poorer images do not have to be saved.

For studying time evolution of solar phenomena, as many artifacts as possible must be removed from the images. A time sequence of images from an excellent groundbased site still exhibits serious artifacts caused by atmospheric distortions even after image selection and removal of gross image motion. Unfortunately, the better the images the more visually disturbing the distortions are to movie observation. Differential image motion across the field of view, "rubber sheet distortion," remains even in images whose sharpness approaches the diffraction limit. Areas of similar distortion are about 3 to 5 arc seconds in extent on the excellent images from the Canary Islands and Pic du Midi. (The small size of the distortion patches is most likely due to weak turbulence at 10 km, and probably should be expected at any excellent ground based site.) Because of the sharpness of the best images, distortions are not clear from single images and are hard to recognize on sequences of prints. However, the difference between movies with and without distortions is remarkable. Fortunately, distortions can be removed from rapid time sequences by procedures which assume that the rapid displacements of distortion patches are

atmospheric rather than solar. Of course, such procedures must be used with some caution because of the possibility of introducing artificial flows into the data in the process of removing distortions. Distortion removal codes are now relatively costly in computer time. “Destretching” a set of 500 512×512 16 bit images takes approximately 30 hours on a Vaxstation 3200.

High resolution observations of the solar surface show a complex array of interacting phenomena – the global oscillations, granulation, mesogranulation, supergranulation, thermal and internal gravity waves, and quasi-stationary flow fields with various scales. Furthermore, all of these properties change with the magnetic field filling factor. To understand the physics of the solar surface, it is essential first to separate these processes.

The data from SOUP showed the importance of the global oscillations in the intensity fluctuations observed in the surface, and how these obscured the evolution of the solar granulation. Figure 3 shows the temporal autocorrelation function (ACF) of the intensity field from groundbased data and SOUP. The agreement is remarkable, especially considering the fact that the spatial resolution varies from about 0.3 arc second in the La Palma data to at least one arc second in some of the other data. Figure 4 further illustrates the robustness of the ACF to resolution by the comparison of the ACF of original (a) and data smeared to one arc second (c). Curves (a) and (c) do not differ significantly. The ACF’s and the movies suggest that the global oscillations play a dominant role in the temporal autocorrelation function.

The spatio-temporal ($k - \omega$) dispersion relation for the global oscillations is well known. It was therefore possible to remove global oscillations from the SOUP data by three dimensional (3D) Fourier transforming from the $x - y - t$ space of the original data to $k_x - k_y - \omega$ space, applying a filter in this space to delete the region of the oscillations, and then inverse transforming back to $x - y - t$ space. Figure 4 (b) and (d) show the ACF functions for the original (a) and degraded (b) image set, respectively, after filtering. Figure 4 demonstrates that the five minute oscillation does dominate the ACF’s and that after the oscillations are removed the difference between original and degraded data is distinct.

Removal of the global oscillations allows the difference between quiet and magnetic Sun to be measured. Figure 5 shows the ACF’s for regions of quiet and magnetic sun (average magnetogram signal greater than 75 gauss) before (a) and (b) and after (c) and (d) Fourier filtering. Before filtering there was some difference between quiet and magnetic ACF’s, but after filtering the $1/e$ decay time differs by nearly a factor of three.

Because of the absence of seeing it was possible to use local correlation tracking (LCT) to follow local displacements of the intensity field in pairs of images and thus infer the horizontal velocities. The spatial resolution of the horizontal velocity measurements is determined by the field-of-view, “mask size,” used for correlation tracking. Since the success of LCT on SOUP data, the technique has been used with great success on ground based data. Using the SOUP horizontal flow measure-

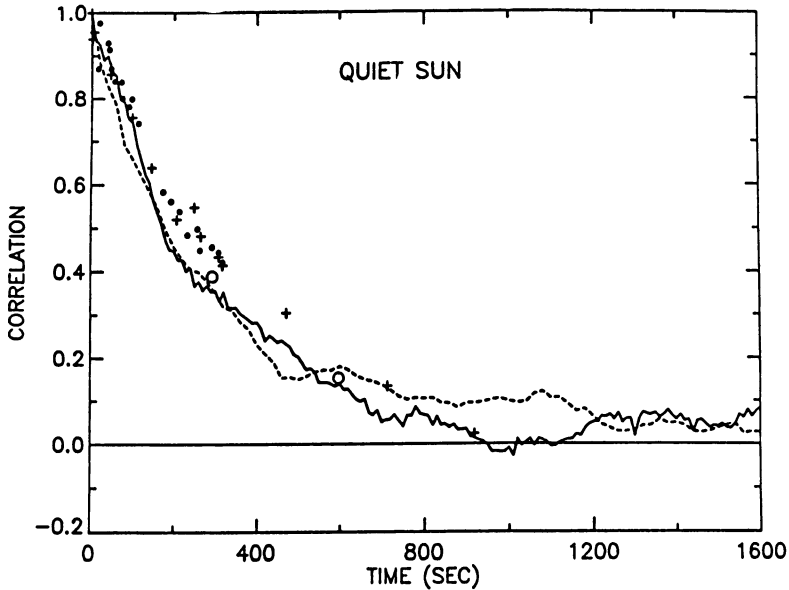


Fig. 3 The temporal autocorrelation function of the intensity field from two different quiet sun regions from SOUP (solid and dashed) and several different groundbased measurements (dots, crosses, and circles).

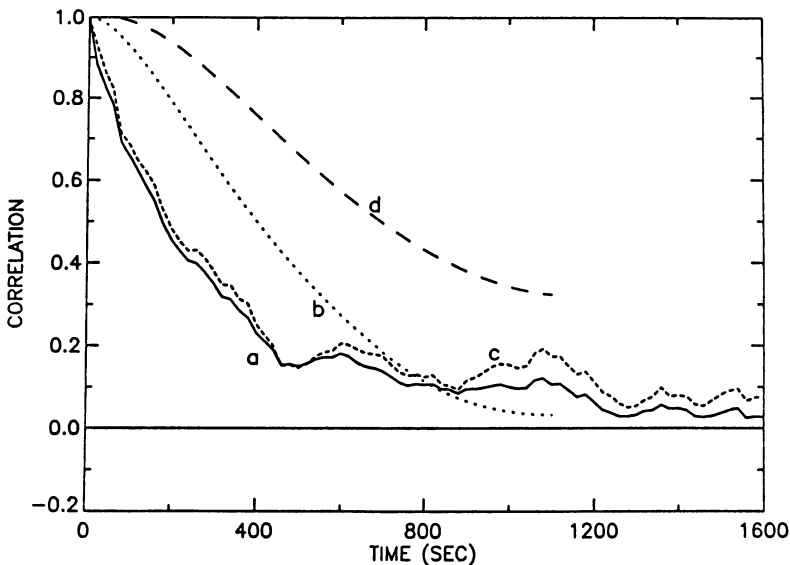


Fig. 4 Autocorrelation functions from 0.134 arc second/pixel SOUP quiet sun for original data (a), the same data Fourier filtered to remove oscillations (b), the same data as (a) smeared to 1 arc second resolution before autocorrelating (c), the same data as (b) smeared to 1 arc second resolution before correlating.

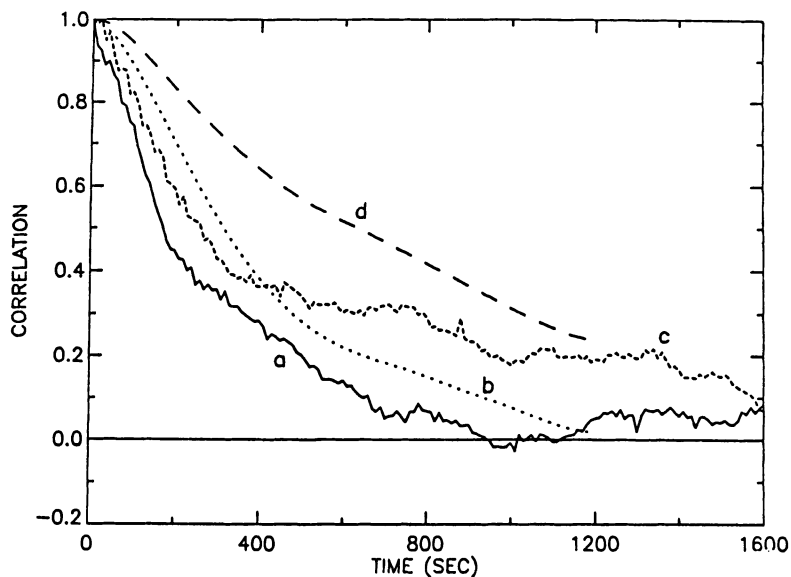


Fig. 5 Autocorrelation functions for quiet sun before (a) and after Fourier filtering (b) and for magnetic sun before (c) and (d) after Fourier filtering.

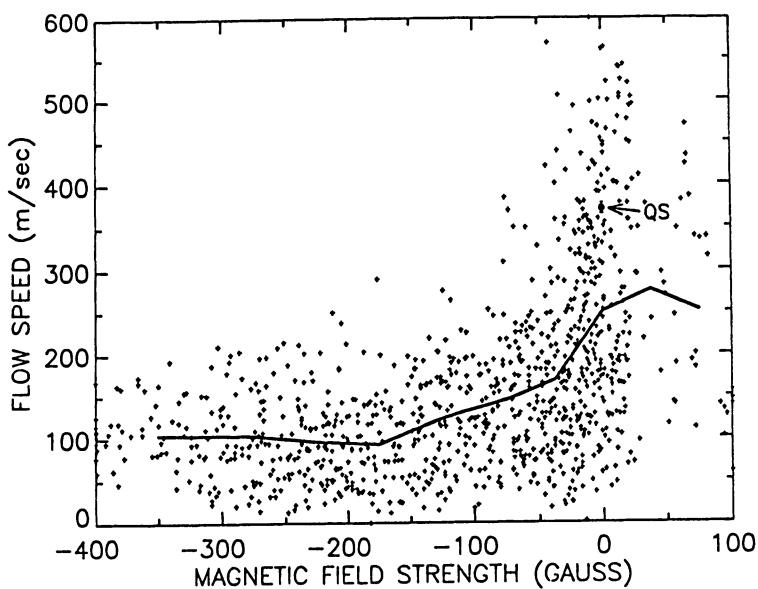


Fig. 6 Scatter plot of horizontal flow speed versus magnetogram signal. The mean flow speed versus magnetogram signal is shown solid. The dot labeled QS is the mean flow speed in zero gauss quiet sun.

ments, most of the decay of the temporal ACF could be explained by the spatial decorrelation of the granulation pattern because of local flows. Figure 6 shows a scatter plot of 25 minute (one orbit) averaged horizontal velocity as measured with a 3 arc second gaussian mask, versus magnetogram signal. In regions of magnetic field, the granulation pattern is advected by flows at a rate a third that in quiet Sun.

The instantaneous horizontal velocities measured by LCT can be used to calculate the RMS velocity fluctuations. Figure 7 shows the RMS velocity versus aperture mask size in regions with different amounts of magnetic flux. In quiet sun, apertures of the size of granulation yield RMS velocities of 1.6 km/s. This is sufficient to account for the width of solar lines. It can be seen from the figure that the vigor of the granulation is suppressed in magnetic regions, but not in regions between field structures.

Once the global oscillations were removed, it was evident from the SOUP movies that exploding granules were a very common phenomenon rather than a reasonably rare occurrence as previously reported. The birth rate and total area covered in the expansion phase is sufficient to cover the solar surface in about 20 minutes. Maps of the divergence of the horizontal flow fields reveal a structure with a mean diameter of about 7 arc seconds. This scale is clearly larger than granulation and smaller than supergranulation and can be fairly represented as mesogranulation. Exploding granules are almost always associated with areas of positive divergence which define the mesogranulation pattern. Thus the two processes are intimately

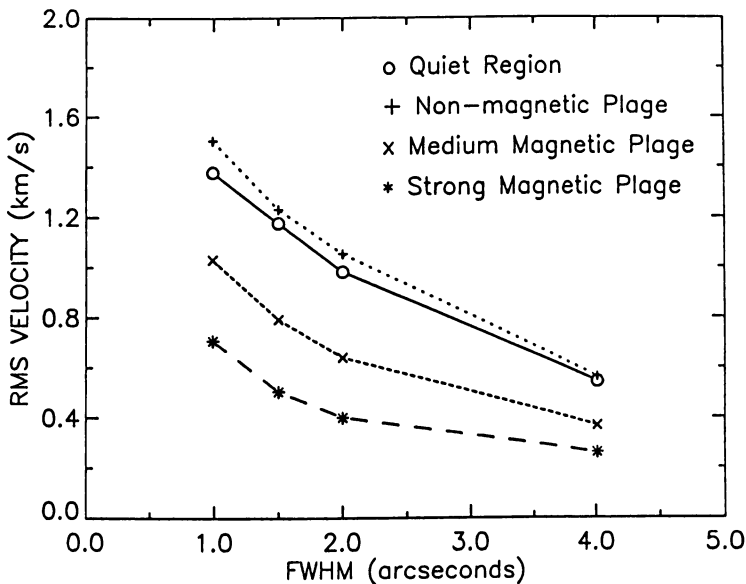


Fig. 7 RMS velocity versus width of the LCT gaussian mask for several different solar regions.

associated.

Measurements based on SOUP, La Palma, and Sacramento Peak data have yielded somewhat different results on mesogranulation inferred from LCT. Direct Doppler measurements from Sacramento Peak and Big Bear observations yield data on the mesogranulation which differ among themselves and with the LCT measurements. The LCT measurements are sensitive to the quality of the original data and the size of the sampling aperture used for the tracking. The Doppler measurements are sensitive to the image quality and time average required to remove 5 minute oscillations. Doppler measurements are also made at a very different height in the atmosphere. We believe that LCT has shown that there is an important flow scale in the photosphere that is larger than granulation with a lifetime on the order of an hour, that enough good data has not yet been reduced to define the flow sufficiently, and that the different interpretations are due to differences in temporal and spatial resolution and analysis procedures.

The existence of a scale larger than granulation in the surface flow is best exhibited by "corks" which are free floating test particles moved by the measured horizontal flow field. Corks are observed to collect in linear structures with a size of 6 to 7 arc seconds in about 30 minutes. Figure 8 shows a set of consecutive 30 minute evolutions of corks that cover 75 minutes. From the figure it is clear that the mesogranular structure evolves on the time scale of an hour.

3. Filtergram Observations

The techniques developed for obtaining and analyzing continuum images have also been applied to narrow band filter images. Because of the longer exposure times and more elaborate optical systems required, the image quality achieved is not as good as that of continuum images but the relative improvement over unstabilized images is great. Figure 9 (a),(b),(c), and (d) show a continuum image, a line center image, a Dopplergram, and a magnetogram taken through a 80 milliangstrom tunable filter. All of the images were taken with exposure times of about 0.3 second using a 1024×1024 Texas Instrument virtual phase CCD.

The images shown in figure 9 are part of a time sequence of three hours duration. Every 50 seconds images were obtained in the blue wing of Fe 6302 Å (-60 mÅ) in right and left circularly polarized light, in four wavelengths through Ni 6768 (-90, -30, 30, 90 mÅ), and in the continuum near Ni 6768 (1500 mÅ). From these data movies have been created of all the wavelength steps, magnetograms, Dopplergrams, and the line center corrected for Doppler shift. All of the images have been corrected for atmospheric distortion and aligned with respect to each other to a fraction of a pixel (one pixel = 0.17 arc second.)

Comparison of the magnetogram, Dopplergram, and line center images in figure 9 shows that the vertical component of the velocity, the size of the of granules, the bright line center structures ("filigree") and the magnetic field are interrelated. In areas where the vertical component of velocity has average amplitude and the granules have their normal 2 arc second spatial structure, the line center bright

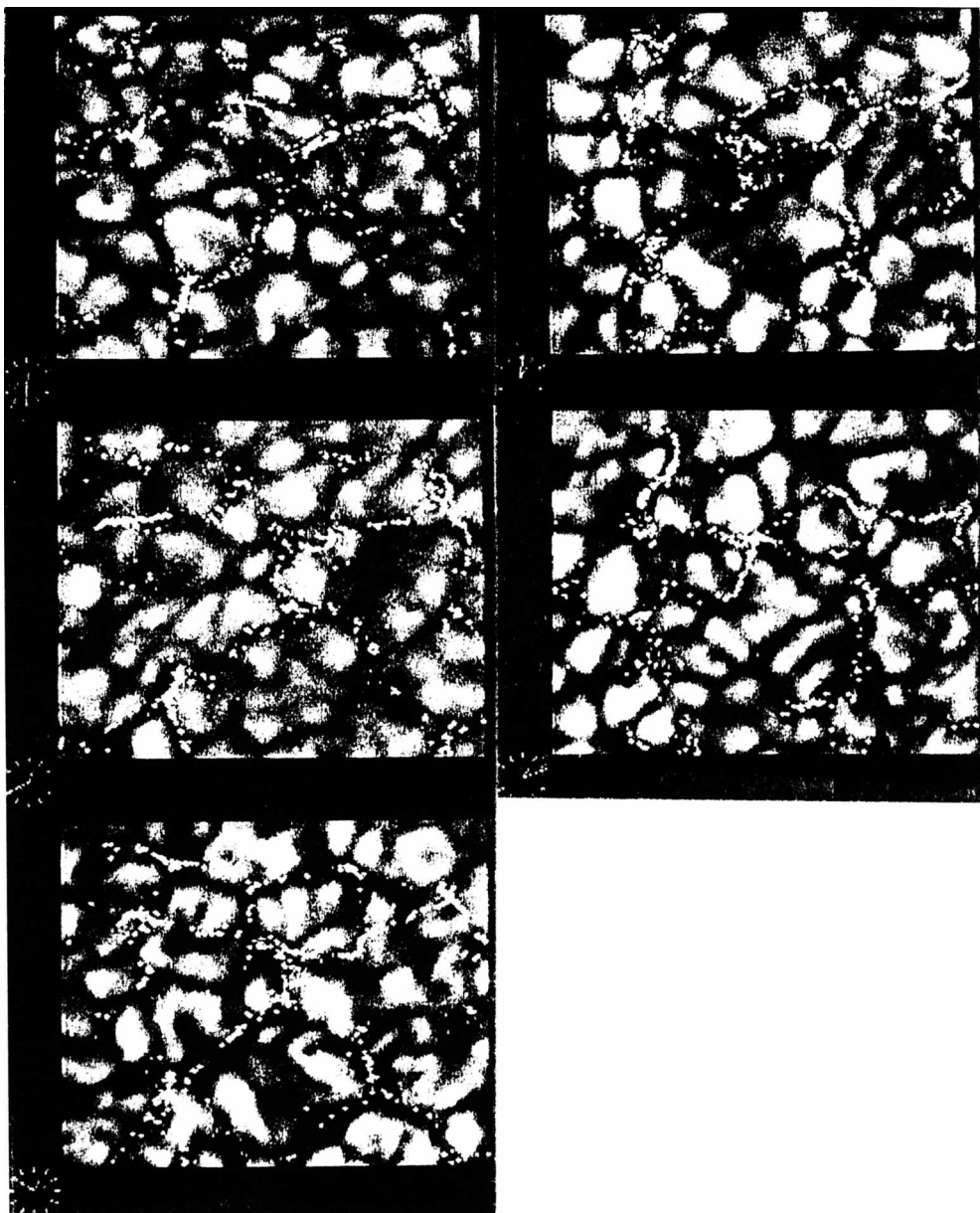


Fig. 8 A set of consecutive 30 minute cork evolutions covering 75 minutes.

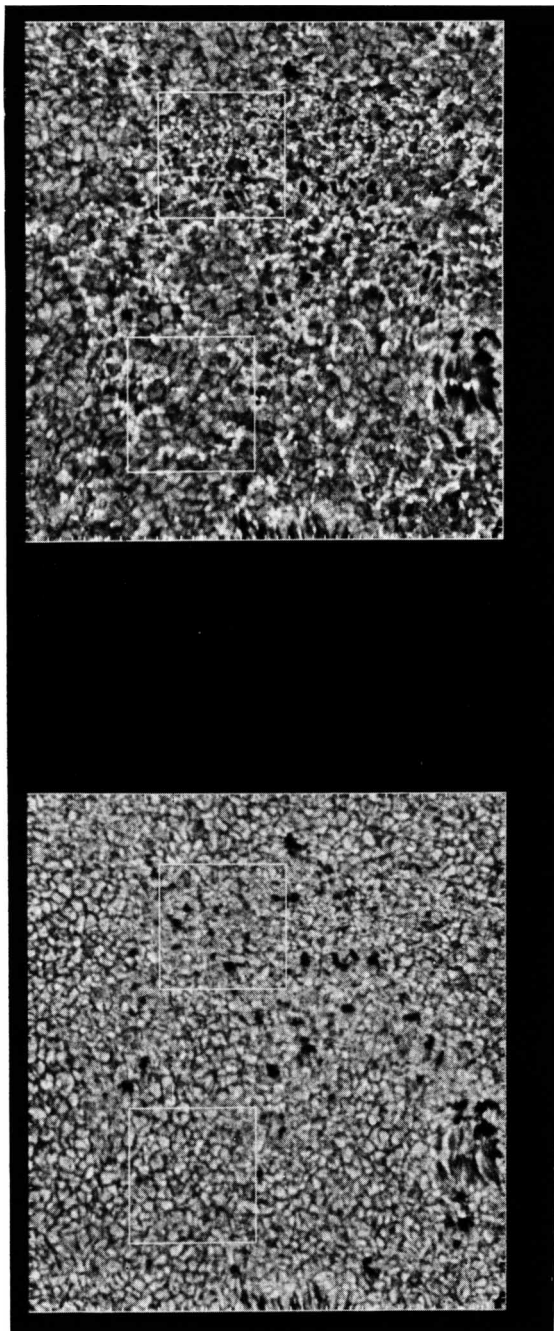


Fig. 9 (a), (b) Continuum image (a) and line center image (b) taken within 50 seconds at SSO through a 80 mÅ tunable filter. The white boxes overlaid on the images are shown expanded in figure 10. Tick marks are at 2 arc second intervals the field of view is 85×85 arc seconds

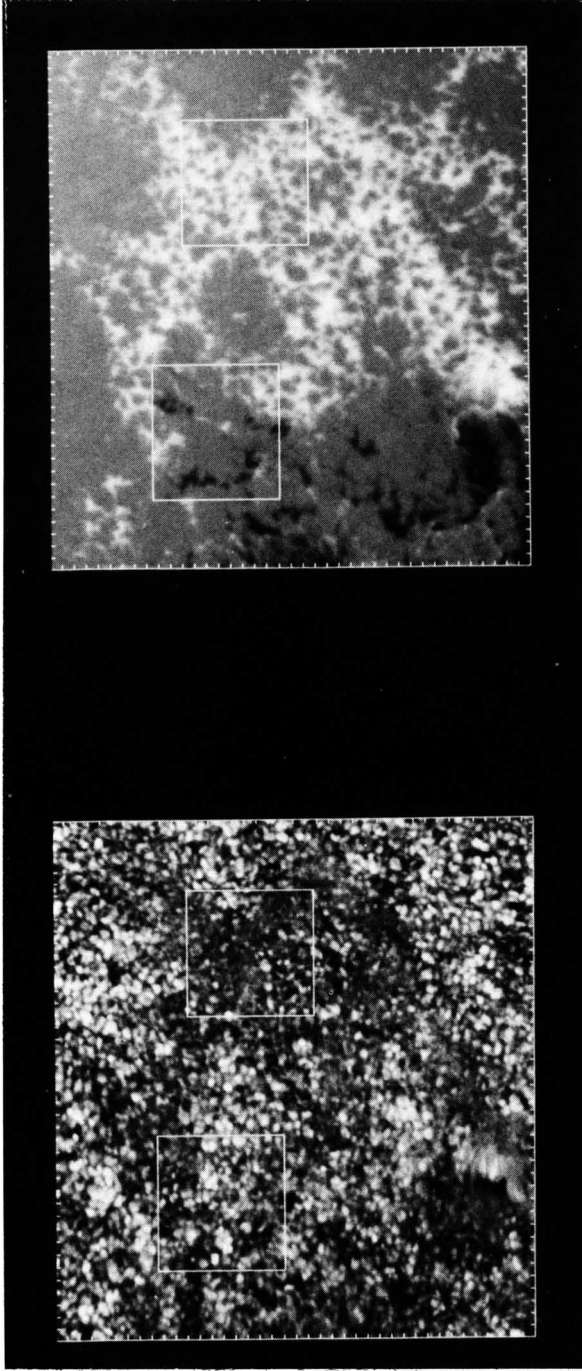


Fig. 9 (c), (d) Dopplergram (c) and a magnetogram (d) taken within 50 seconds at SSO through a 80 mÅ tunable filter. The white boxes overlaid on the images are shown expanded in figure 10. Tick marks are at 2 arc second intervals the field of view is 85 × 85 arc seconds

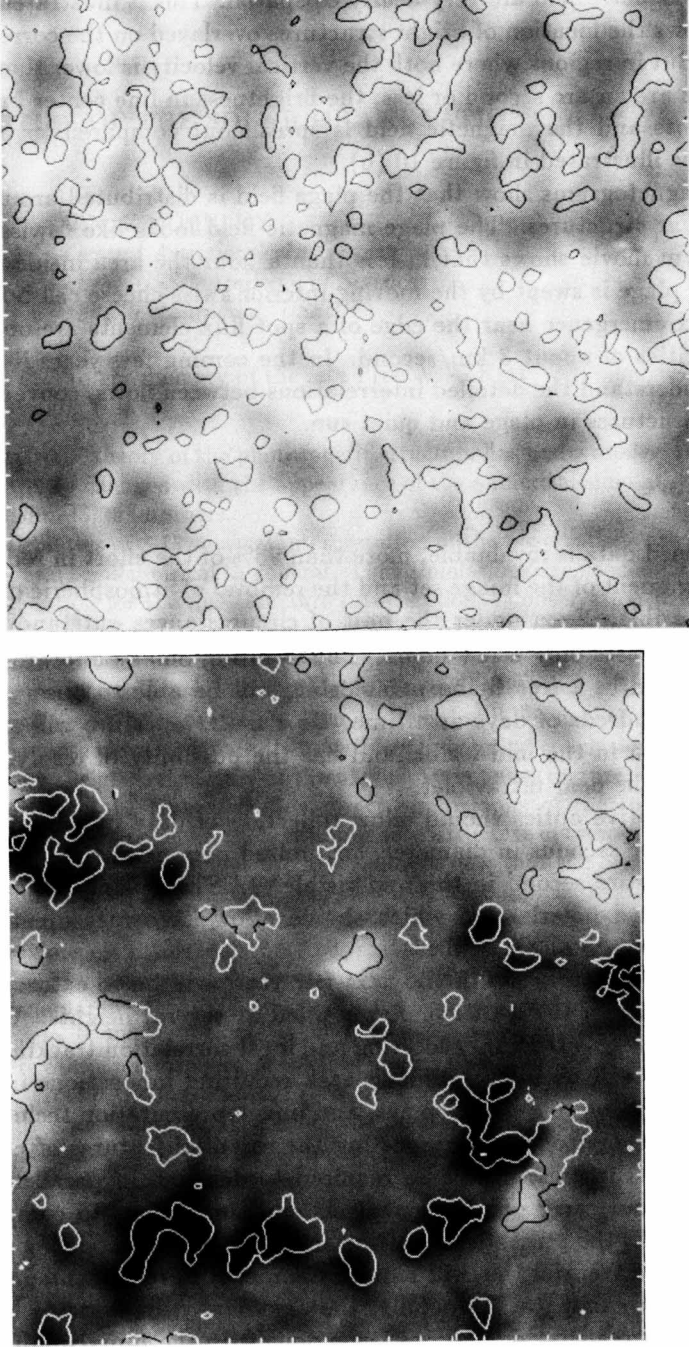


Fig. 10 Magnetograms from regions where the Doppler signal is average (a) and lower than average (b). Overlaid on the magnetograms are contours of the line center bright points. The locations of the magnetograms are marked on the images in figure 9. The tick marks are at 1 arc second intervals.

structures and magnetic field are very nearly co-spatial. This is illustrated in figure 10 (a) which shows the location of bright structures overlayed on the corresponding magnetogram. But in regions where both the vertical velocity is lower than average and the granules are an arc second or less, the brightness in line center breaks into many small points and the magnetic field is spread out compared to brightness structure. This is illustrated in figure 10 (b).

Individual magnetograms show that the plage field is distributed around 2 to 5 arc second cellular structures. The plage magnetic field looks like "swiss cheese." The magnetogram movie shows that in less than a hour the area inside the outer boundary of the plage is swept by the moving interior swiss cheese cell boundaries. In regions of flux emergence near the edge of a spot flux elements are observed to move with velocities of about 3 km/second. In the coming few years it will be a major task to understand the detailed interrelations between flows, convection, and magnetic field structures in plage and quiet sun.

4. For the Future

While ground based data is invaluable, more than 95% of the effort in reducing the data is in the alignment of the image set and the removal of atmospheric distortions to the extent possible. Even under the best of circumstances outstanding seeing – 1/3 arc second – lasts only a few hours. The Orbiting Solar Laboratory (OSL), which will be placed in a free flying polar orbit, will be able to observe the sun continuously for hundreds of days at a time. Its 1 meter aperture will allow 1/10 arc second resolution in the mid-visible and has the possibility of resolving nearly 1/20 arc second in the near ultraviolet.

LEST using adaptive optics should allow collection of data in a limited region of the sun, 2 to 5 arc seconds in diameter, for limited periods of time, hours, with a resolution of 1/25 arc second in the mid-visible. LEST is being designed to be nearly free of induced polarization which should allow it to measure the vector magnetic fields of very small flux tubes.

A major task for solar physics in the next few years will be to extract physical processes from movies of the atmosphere obtained at several heights. Compared with the development of 3-D Fourier filtering and local correlation tracking of granulation movies, this will be a very difficult task requiring innovations in analysis procedures, manipulation of video displays, and image presentation techniques.

As techniques are developed for extracting the essential features of convection and magnetic fine structures, it will be required to develop, in parallel, detailed theoretical models and carry out both analysis and simulations to compare with the measurements. At the present state of the art in convection modeling and three dimensional radiative transfer this will require significant developments in the very largest computers in existence. Hopefully, the next few years will see new ideas emerge which permit realistic simulations to be done with the supercomputers then available.